Angiotensinergic stimulation of vascular endothelium in mice causes hypotension, bradycardia, and attenuated angiotensin response

Ramaswamy Ramchandran*, Takanobu Takezako*, Yasser Saad*, Linda Stull†, Bruno Fink‡, Hirotsugu Yamada†, Sergey Dikalov‡, David G. Harrison‡, Christine Moravec†, and Sadashiva S. Karnik*§

*Department of Molecular Cardiology, Lerner Research Institute, and †Department of Cardiovascular Medicine, Cleveland Clinic Foundation, Cleveland, OH 44195; and ‡Division of Cardiology, Emory University School of Medicine, Atlanta, GA 30322

Edited by Thomas M. Coffman, Duke University and Durham Veterans Affairs Medical Centers, Durham, NC, and accepted by the Editorial Board October 19, 2006 (received for review April 4, 2006)

It is not clear whether endothelial cell (EC) activation by the hormone angiotensin II (Ang II) modulates contraction of vascular smooth muscle cells (VSMCs) in the vasculature and whether impairment of this regulation *in vivo* contributes to hypertension. Delineation of the actions of Ang II through the type 1 receptor (AT1R) on ECs in the blood vessels has been a challenging problem because of the predominance of the AT1R functions in VSMCs that lie underneath the endothelium. We have obviated this limitation by generating transgenic (TG) mice engineered to target expression of the constitutively active N111G mutant AT1R only in ECs. In these TG mice, the enhanced angiotensinergic signal in ECs without infusion of Ang II resulted in hypotension and bradycardia. The pressor response to acute infusion of Ang II was significantly reduced. Increased expression of endothelial nitric oxide synthase and production of hypotensive mediators, nitric oxide and cyclic guanosine monophosphate, cause these phenotypes. Hypotension and bradycardia observed in the TG mice could be rescued by treatment with an AT1R-selective antagonist. Our results imply that the Ang II action by means of EC-AT1R is antagonistic to vasoconstriction in general, and it may moderate the magnitude of functional response to Ang II in VSMCs. This control mechanism *in vivo* most likely is a determinant of altered hemodynamic regulation involved in endothelial dysfunction in hypertensive cardiovascular disease.

angiotensin II receptor | endothelial nitric oxide synthase | hypertension | nitric oxide | angiotensin receptor blockers

The octapeptide hormone angiotensin II (Ang II) mediates homeostatic control of the renin–angiotensin system (RAS) in the regulation of vascular tone, water–electrolyte balance, and cardiac function through the G protein-coupled Ang II type 1 receptor (AT1R) (1). Binding of Ang II and activation of AT1R on vascular smooth muscle cells (VSMCs) are extremely potent vasopressor stimuli, acutely raising blood pressure by increasing vascular resistance. Multiple hemodynamic, hormonal, and neuronal control mechanisms *in vivo* moderate the vasoconstrictor tone of Ang II on the vasculature, and among them endothelium-derived vasorelaxation is vital. However, direct regulation of this mechanism by Ang II is not clearly established.

Increased capacity of VSMCs to bind Ang II is known to accelerate vascular lesion formation in animals. Preventing Ang II formation and Ang II binding to tissue targets significantly reduces hypertension, atherosclerosis, and heart failure in both humans and animals (1–3). Functional AT1Rs are present on endothelial cells (ECs), but their overall importance in physiology is unclear (4–6). However, the consequence of AT1R activation in ECs is not clearly established in normal physiology and in the pathophysiology of hypertensive diseases. Cell culture studies (7, 8) indicated that EC-AT1R stimulation produces vasodilator substances. But studies in isolated blood vessels were inconclusive with regard to an Ang II-dependent modulation of vascular tone by ECs depending on the vessel studied (9–11). The lack of experimental models targeting AT1R function specifically in ECs is a major obstacle. Consequently, the hypothesis that EC-AT1R moderates vasoconstriction mediated by VSMCs (12, 13) and impairment of this regulation leads to hypertension has not yet been critically tested.

The low density of EC-AT1R and the relative dominance of VSMC-AT1R in vasculature render the study of functional attributes of EC-AT1R technically challenging. We attempted to overcome this limitation by generating transgenic (TG) mice in which the EC is the target of direct angiotensinergic stimulation. We used the Tie1 promoter (14) to drive EC-specific expression of the constitutively active mutant of the rat AT1R transgene (15) (Fig. 1*A*). We used the single mutant, N111G, which spontaneously activates intracellular calcium mobilization (15–17). This mutant can be fully activated by the Ang II analog [Sar^1,Ile^4,Ile^8]Ang II (SII-Ang II), which does not activate the native AT1R and is fully inhibited by the AT1R inverse agonist, L-158809 [see supporting information (SI) Fig. 6]. The Tie1-AT1R TG mice displayed hypotension, bradycardia, attenuated pressor response to infused Ang II, increased blood and tissue nitric oxide (NO), and elevated endothelial nitric oxide synthase (eNOS) and cGMP. The resulting symptoms in the TG mice could be rescued with the AT1R blocker L-158809. Our findings suggest a vasodilatory role for EC-AT1R.

Results

Tie1-AT1R$_{N111G}$ Transgene-Expressing Mice. We identified three founder mice with the integrated Tie1-AT1R$_{N111G}$ transgene (Fig. 1*A*). The Southern blot band intensity was used to estimate heterozygous transgene copy numbers of 18, 10, and 1 in founder lines TG6, TG23, and TG26, respectively (Fig. 1*B*). We then determined the expression of transgene mRNA in F1 and F2 generation heterozygotes by RT-PCR analysis of poly(A)$^+$ RNA prepared from tissues. Of the three transmitting founder lines, TG23 and TG26 showed transgene expression, whereas the TG6 line did not. Real-time quantitative RT-PCR was used to estimate the proportion of endogenous AT1R to TG transcript levels in several tissues in the TG23+/− (Fig. 1*C*) and TG26+/− (data not

Author contributions: R.R. and T.T. contributed equally to this work; R.R., T.T., C.M., and S.S.K. designed research; R.R., T.T., Y.S., L.S., B.F., H.Y., C.M., and S.S.K. performed research; R.R., S.D., D.G.H., C.M., and S.S.K. contributed new reagents/analytic tools; R.R., T.T., and S.S.K. analyzed data; and R.R., T.T., and S.S.K. wrote the paper.

The authors declare no conflict of interest.

This article is a PNAS direct submission. T.M.C. is a guest editor invited by the Editorial Board.

Abbreviations: Ang II, angiotensin II; AT1R, Ang II type 1 receptor; BAEC, bovine aortic endothelial cell; CCF, Cleveland Clinic Foundation; EC, endothelial cell; eNOS, endothelial nitric oxide synthase; NO, nitric oxide; NT, nontransgenic; NTL, nontransgenic littermate; RAS, renin–angiotensin system; SII-Ang II, [Sar^1,Ile^4,Ile^8]Ang II; TG, transgenic; VSMC, vascular smooth muscle cell.

§To whom correspondence should be addressed. E-mail: karniks@ccf.org.

This article contains supporting information online at www.pnas.org/cgi/content/full/0602715103/DC1.

© 2006 by The National Academy of Sciences of the USA

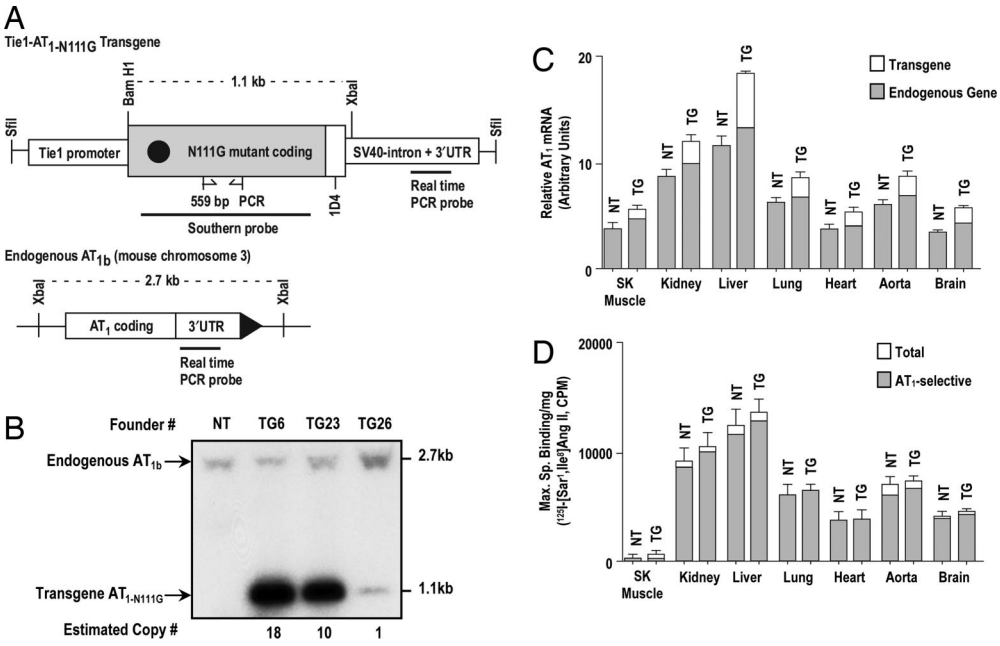

Fig. 1. General characterization of the Tie1-AT1R TG mice. (*A*) Transgene construct that was injected in to mouse oocytes. The 735-bp-long EC-specific mouse Tie1 promoter, AT1R synthetic gene in which the codon for the residue Asn[111] was mutated to Gly[111], the 1D4 epitope tag, and the intron+ 3′ UTR of the SV40 T antigen are depicted. The C-terminal 1D4 epitope distinguishes transgene AT1R from the endogenous AT1R (15). A representation of restriction map of the mouse AT_{1b} gene is shown. The sites for binding genotyping primers, Southern probe, and transgene transcript-specific real-time PCR probe are shown with the site of binding for the real-time PCR probe, which is specific for native AT1R mRNAs. (*B*) Southern blot analysis of genomic DNA digested with BamHI and XbaI from nontransgenic (NT) and transmitting TG founder mice. The probe hybridizes to 2.7- and 1.1-kb fragments, which represent the endogenous AT_{1b} gene and the transgene, respectively. The XbaI–BamHI fragment of the AT_{1a} gene (5.9 kb) does not appear on the gel shown. (*C*) Quantitative real-time PCR estimation of levels of total AT1R mRNA and endogenous AT1R mRNA (shaded fraction) in poly(A)$^+$ RNA isolated from TG23+/− mice compared with NT. (*D*) Maximum specific binding (B_{max}) of the ^{125}I-[Sar^1,Ile^8]Ang II in membranes purified from various tissues from TG23+/− mice compared with NT mice. The shaded fraction in each bar represents the AT1R-selective binding in each tissue; the remaining binding may be caused by the AT_2 receptor. Error bars represent SEM. ($n > 3$ for each tissue). SK Muscle, skeletal muscle.

shown). The endogenous AT1R expression in TG23+/− (Fig. 1*C*) and TG26+/− (data not shown) were not significantly different from NT littermates (NTL). The transgene mRNA levels in the TG23+/− were ≈3-fold higher than that in the TG26+/− in all tissues examined.

We compared the AT1R protein expression in NTL and the TG23+/− (Fig. 1*D*) by saturation-binding analysis of membranes prepared from various tissues. As anticipated, skeletal muscle showed low specific ^{125}I-Ang II-binding (receptor density) values in all mice. The distribution and magnitude of AT1R expression in TG23+/− were not significantly different from those in the NTL. The EC-rich tissues, liver, lungs, and kidneys, from TG23+/− mice had consistently higher specific binding values than the NTL (Fig. 1*D*). These findings are expected, given that the majority of ^{125}I-Ang II binding in tissues is caused by AT1R abundance in nonendothelial cells, which makes it difficult to estimate the level of transgene overexpression in ECs in the TG mice. However, the results shown in SI Fig. 7 suggest that N111G receptors constitute ≈25 and 40% of the total AT1R in the ECs of newborn TG23+/− and TG26+/− mice, respectively. We conclude that the transgene expression causes a modest increase of AT1R level.

EC-Specific Transgene Expression. Immunohistochemical staining of the transgenic AT1R protein in TG23+/− (Fig. 2) and TG26+/− lines (data not shown) showed expression in ECs lining the microvasculature of the kidneys and lungs of adult mice. TG AT1R immunostaining was absent in the ECs of large vessels. This pattern of expression was previously reported for the Tie1-β-gal reporter gene (14). The TG receptor protein is specifically identified by the presence of an epitope tag (Fig. 1*A*) that is recognized by the anti-ID4 antibody as shown earlier (15).

General Characterization of Phenotype. Heterozygous TG23 and TG26 mice were viable, and no gross phenotypic or histologic abnormalities were seen in kidneys, liver, lungs, spleen, heart, and brain. We therefore attempted to establish homozygous colonies for each of the founder lines by breeding F2 generation heterozygotes. The F2 generation crosses produced no TG23+/+ (in >25 crosses) and a smaller number of TG26+/+ litters, making propagation of TG26+/+ somewhat difficult. Hence, we used heterozygous mice for most of the analyses of the phenotype. The nonexpressing TG6+/+ were readily obtained with a litter size similar to that of NT mice. NT and TG6+/+ lines had a survival rate of >98% at 18 months. The survival rates for TG23+/−, TG26+/−, and TG26+/+ mice varied, 60–95% at 18 months. The reasons for increased mortality are unclear. No significant visible phenotypic differences were apparent in the TG mice at 4–6 months-of-age (Table 1).

Blood Pressure and Vascular Response. At 5 months of age, systolic blood pressure measured in conscious animals was significantly reduced in all TG lines (TG26+/−, 116 ± 2 mmHg (1 mmHg = 133 Pa); TG26+/+, 113 ± 2 mmHg; TG23+/−, 112 ± 2 mmHg; NTL, 129 ± 2 mmHg; $P < 0.05$) (Fig. 3*A*). Both male and female TG were hypotensive. Pearson's correlation coefficient evaluation of the

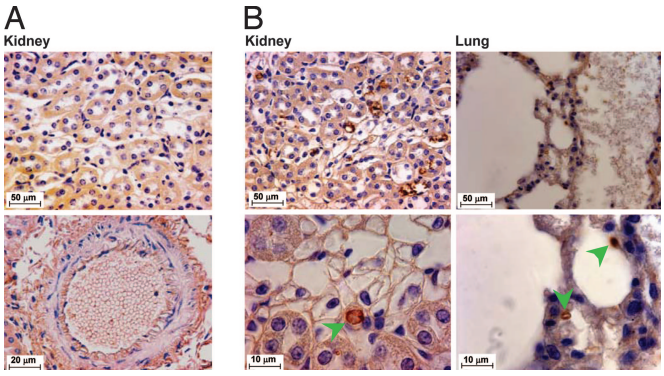

Fig. 2. Localization of TG AT1R protein in the endothelium. Immunohistochemical staining of sections of the indicated tissues from NT and TG23+/− mice with 1D4 epitope-specific rabbit polyclonal antibody is shown. (Scale bars: *Upper*, 50 μm; *Lower*, 10 μm.) Arrows indicate 3,3′-diaminobenzidine staining localized to microvasculature.

Table 1. Physiological parameters, cardiac function, and biochemical data of 5-month-old mice

Parameter	NT (*n*)	TG26+/− (*n*)	TG23+/− (*n*)
Body weight, %	100 ± 2 (8)	98 ± 3 (7)	100 ± 3 (8)
Systolic blood pressure, mmHg	129 ± 1 (18)	116 ± 3 (17)**	112 ± 2 (18)**
Heart rate, bpm	737 ± 5 (8)	694 ± 18 (7)*	688 ± 19 (8)*
Heart weight, mg/g of body weight	5.58 ± 0.1 (30)	5.74 ± 0.19 (16)	5.39 ± 0.19 (22)
LV mass, mg/g of body weight)	2.70 ± 0.13 (16)	2.95 ± 0.18 (12)	2.96 ± 0.18 (13)
Fractional shortening, %	52.2 ± 2.2 (16)	49.0 ± 2.2 (12)	57.9 ± 1.5 (13)
Heart ANP/GAPDH transcript	0.8 ± 0.1 (8)	0.9 ± 0.1 (6)	0.8 ± 0.1 (6)
Heart ANP, pg/mg of protein	152 ± 11 (8)	163 ± 19 (6)	153 ± 19 (6)
Plasma urea nitrogen, mg/ml	19.6 ± 1.2 (8)	20 ± 0.9 (6)	20.4 ± 1.1 (8)
Plasma creatinin, mg/ml	0.14 ± 0.02 (8)	0.15 ± 0.02 (6)	0.14 ± 0.02 (8)
Plasma sodium, mmol/liter	165.1 ± 1.1 (8)	166.3 ± 2.5 (6)	162.6 ± 1.6 (8)
Plasma potassium, mmol/liter	7.0 ± 0.4 (8)	6.7 ± 0.2 (6)	6.6 ± 0.5 (8)
Plasma chloride, mmol/liter	116.5 ± 0.7 (8)	115.7 ± 0.8 (6)	114.5 ± 1.2 (8)
Blood NO, μM	0.71 ± 0.03 (15)	0.89 ± 0.05 (12)*	0.99 ± 0.11 (12)*
Plasma ET-1, pg/ml	3.85 ± 0.29 (8)	3.36 ± 0.16 (6)	3.73 ± 0.24 (8)
Plasma renin activity, ng Ang I per ml/h	11 ± 4 (8)	13 ± 6 (6)	14 ± 5 (6)
cGMP in plasma, pmol per 100 μl)	3.81 ± 0.58 (6)	4.39 ± 0.45 (6)	—
cGMP in aorta, fmol/mg of protein	40 ± 2 (8)	71 ± 6 (6)**	83 ± 4 (8)**

The number of samples are shown as (*n*). Values are expressed as mean ± SEM. *, $P < 0.05$; **, $P < 0.01$ vs. control. LV mass, left ventricular mass; bpm, beats per minute; ET-1, endothelin-1; ANP, atrial natriuretic peptide; —, not examined.

association between body weight and systolic blood pressure indicated that the hypotension observed in the TG is not caused by variability in body weight. Acute infusion of 1 μg of Ang II per kg of body weight demonstrates that carotid arterial pressure response is depressed 41% in TG23+/− and 55% in TG26+/− compared with NTL ($P < 0.05$) (Fig. 3*B*). The difference between TG23+/− and TG26+/− lines is not significant. Infusion of the AT1R blocker L-158809 before Ang II completely abolished the acute Ang II response (data not shown), demonstrating AT1R specificity of the response. However, response to infusion of the eNOS inhibitor L-NAME in these mice was similar to that in NTL (data not shown).

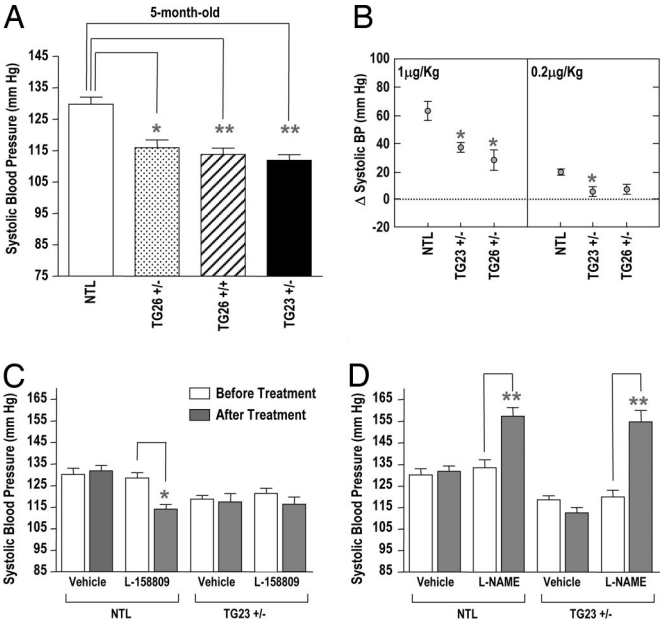

Fig. 3. Hypotension in the Tie1-AT1R TG mice. (*A*) Tail-cuff blood pressure-measurement. Systolic blood pressure is represented in a 5-month-old group of mice, NTL, $n = 18$; TG26+/−, $n = 18$; TG26+/+, $n = 18$; and TG23+/−, $n = 18$; *, $P < 0.05$; **, $P < 0.01$ vs. NT mice. NTLs were combined from different lines, and their blood pressure did not differ. (*B*) Acute effects of Ang II infusion on blood pressure. A change in carotid artery pressure with infusion of 1 μg or 0.2 μg of Ang II per kg of body weight was measured in anesthetized 6-month-old TG23+/−, TG26+/−, and age-matched NTL ($n = 6$; *, $P < 0.05$ vs. NTL). (*C*) Effect of 4-week treatmentof AT1R antagonist L-158809 (0.025 mg/ml) in drinking water on blood pressure in NTL and TG23+/− mice ($n = 8$). Bars show mean values ± SEM; **, $P < 0.01$. The K_d of L-158809 for the endogenous AT1R is 2.6 ± 0.1 nM, and the K_d for the N111G receptor is 46 ± 5 nM. (*D*) Effect of 4-week treatment with NOS inhibitor L-NAME (1 mg/ml) in drinking water on blood pressure in TG23+/− mice and NTL ($n = 7$). Bars show mean values ± SEM; **, $P < 0.01$.

The heart rate in TG26+/− and TG23+/− lines is significantly reduced (694 ± 18 in TG26+/− and 688 ± 19 in TG23± compared with 737 ± 5 in NTL; $P < 0.05$), but the cardiac functions assessed by echocardiography are normal (Table 1 and SI Figs. 8 and 9). We attempted to block the receptor activity in TG23+/− mice by treatment with the AT1R-selective antagonist L-158809 (Fig. 3*C*). As expected, the drug reduced the blood pressure in NTL (129 ± 3 mmHg before and 114 ± 2 mmHg after treatment; $P < 0.01$). The blood pressure in the TG23+/− remained steady without a significant reduction (116 ± 2 mmHg before and 115 ± 3 mmHg after) (Fig. 3*C*). The heart rate of TG23+/− mice (688 ± 19) improved to 730 ± 20 ($n = 8$) after the treatment, a value that is similar to NTL (see Table 1). Thus, the AT1R antagonist abolished the hypotensive effect and bradycardia observed in TG23+/−. Drinking water containing L-NAME (1 mg/ml) given to NTL and TG23+/− mice increased blood pressure to a similar level in both lines (NTL, 130 ± 4 mmHg before and 154 ± 3 mm Hg after treatment; TG23+/−, 115 ± 3 mmHg before and 155 ± 5 mmHg after treatment) (Fig. 3*D*). However, bradycardia in TG23+/− was not altered by this treatment (data not shown).

Blood NO Levels and Tissue Expression of eNOS. The reduction of blood pressure was accompanied by an elevated NO concentration in blood and eNOS activity in the aorta of the TG mice (Fig. 4 and Table 1) compared with NTL. The blood NO concentration was elevated (Fig. 4*A*) in TG lines (0.99 ± 0.11 μM in TG23+/− and 0.89 ± 0.05 μM in TG26+/− compared with 0.71 ± 0.03 μM in NTL; $P < 0.05$). Elevated blood NO concentration in TG23+/− and TG26+/− is associated with elevated activity of eNOS in the aorta (Fig. 4*B*). The NOS activity was significantly higher in TG23+/− and TG26+/− (0.38 ± 0.04 and 0.36 ± 0.05 pmol/mg of protein per min, respectively; $P < 0.05$) compared with NTL (0.21 ± 0.04 pmol/mg of protein per min). By Spearman's rank correlation, the eNOS activity as well as blood NO concentration appear to be significantly associated with transgene copy number ($P < 0.05$). The blood NO level significantly decreased (Fig. 4*C*),

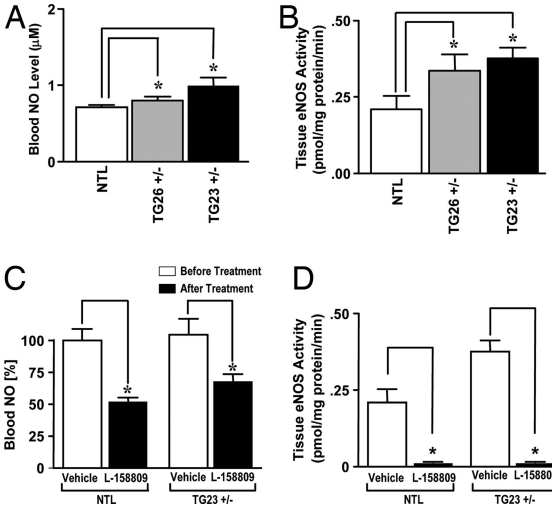

Fig. 4. Mechanism of elevated NO in the Tie1-AT1R TG mice. (*A*) Blood NO level in 4-month-old NTL, TG26+/−, and TG23+/− mice ($n = 10$; *, $P < 0.05$). (*B*) NOS activity measured in the aortic homogenates from NTL, TG26+/−, and TG23+/− mice ($n = 10$; *, $P < 0.05$). Citrulline formation from arginine was determined in the presence (total NOS) and absence inducible NOS (iNOS) of free Ca^{2+}; eNOS activity was calculated by subtracting iNOS from total activity for each individual animal. (*C*) Ability of L-158809 (0.025 mg/ml in drinking water) to rescue TG23+/− mice from the ''elevated NO'' phenotype after a 4-week treatment. The blood NO level was significantly reduced in both NTL and TG23+/− mice ($n = 10$; *, $P < 0.05$). (*D*) Suppression of eNOS activity in the aortic homogenates after 4-week treatment with L-158809 (0.025 mg/ml in drinking water) ($n = 10$; *, $P < 0.05$).

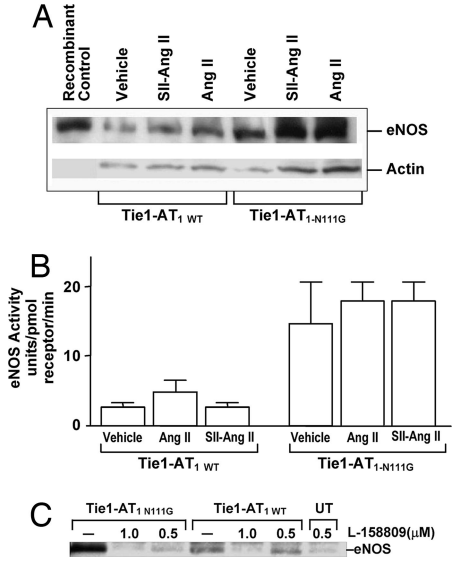

Fig. 5. Effect of AT1R on eNOS expression and activity. (*A*) Expression of eNOS protein in BAECs transfected with either WT or the N111G mutant AT1R expression plasmid after 1 μM Ang II or SII-Ang II treatment for 24 h. Control is recombinant eNOS purified from insect cells. (*B*) Effect of 1 μM ligand stimulation of AT1R for 45 min on eNOS activity. Enzymatic activity of eNOS in WT and N111G mutant AT1R-transfected BAEC lysates ($n = 3$) is shown. Bars show mean ± SEM. (*C*) AT1R specificity of eNOS protein expression in BAEC is demonstrated by treatment with L-158809; UT indicates untransfected BAEC.

and the NOS activity was completely inhibited (Fig. 4*D*) in both NTL and TG23+/− mice by 4-week treatment with the AT1R antagonist L-158809 (0.025 mg/ml). The cGMP was higher in the TG26+/− plasma, although the level of increase did not achieve significance (Table 1). However, cGMP levels in the homogenates from aorta of TG26+/− and TG23+/− are significantly higher than NTL (Table 1), suggesting that the NO target enzyme, soluble guanylate cyclase, is activated in TG mice.

The plasma concentration of ANP, renin, and endothelin-1 was not significantly different between among lines (Table 1). The cardiac levels of ANP peptide and transcripts were not significantly different (Table 1). Furthermore, the indicators of oxidative stress, such as peroxynitrite formation, up-regulation of NOSIII, down-regulation of soluble guanylate cyclase, and atherosclerosis, are absent in these TG mice.

AT1R-Induced Expression of eNOS. Based on the hypotensive phenotype of TG23 and TG26 mice, we anticipated that infusion of SII-Ang II, a selective agonist for the N111G mutant AT1R, would evoke acute vasodilatation and hypotension in TG26+/− and TG23+/−, but not in NT mice. However, acute infusion of SII-Ang II did not evoke both responses (data not shown) in experiments similar to those described in Fig. 3*B*. This observation suggested to us that chronic action of the EC-AT1R in ECs is responsible for the observed hypotension and attenuated Ang II response in TG.

The acute and chronic effects of AT1R on eNOS protein expression and activity were evaluated in transfected bovine aortic ECs (BAECs; Fig. 5). The influence of comparable levels of wild-type (WT) (B_{max}, 1.1 pmol/mg) and N111G mutant (B_{max}, 0.89 pmol/mg) AT1R on steady-state levels of eNOS protein is shown in Fig. 5*A*. The eNOS protein expression level was higher in the N111G mutant-transfected cells compared with the WT. Treatment with Ang II for 24 h increased the eNOS in cells transfected with WT and N111G. In contrast, treatment with SII-Ang II did not increase eNOS in WT, but it did increase eNOS in N111G-transfected cells (Fig. 5*A*). Increased eNOS expression was abolished after treatment with L-158809 in both WT and N111G-transfected cells (Fig. 5*C*). Selective activation of the N111G mutant receptor by SII-Ang II in inositol phosphate production in COS cells was reported earlier (15) (see SI Fig. 6).

Activation with Ang II and SII-Ang II for 45 min did not increase the eNOS activity in either WT or N111G mutant-expressing cells (Fig. 5*B*). However, Ang II treatment produced a 2.5-fold increase in the inositol phosphate production in both the WT and N111G mutant transfected ECs. Treatment with SII-Ang II produced a 1.6-fold increase in inositol phosphate production in the N111G mutant-transfected ECs, similar to an earlier observation in COS-1 cells (15). As expected, the WT receptor was not activated by SII-Ang II. Together, these results demonstrate that AT1R in the activated state increases the steady-state level of eNOS protein in the EC. Altering the steady-state expression of eNOS in ECs by eNOS gene manipulation was previously shown to cause hypotension (18).

Discussion

Our data elucidate a previously unidentified role in EC-AT1R Ang II control of vascular functions. The activated AT1R in ECs promoted eNOS expression and vasodilation, thus restraining the constriction (Ang II-induced) of VSMCs in regulating normal blood pressure. The TG mice expressing a constitutively activated $AT_{1\text{-}N111G}$ mutant receptor under EC-specific Tie1 promoter allowed angiotensinergic activation of ECs specifically, without a generalized AT1R activation, i.e., by augmenting Ang II levels *in vivo*. Endothelial-specific transgene expression using the murine Tie1 gene promoter construct has been reported in refs. 14 and 19. The β-galactosidase reporter gene expression, driven by the 0.8-kb Tie1 promoter, was restricted to the vascular endothelium and microvessels of the kidneys, lungs, and brain, but it was weak in the heart, large conduit vessels, and liver of adult mice (14). We obtained two transmitting founder Tie1-AT1R TG mice (Fig. 1*B*). Both lines maintain the transgene expression throughout life span, and no change was found over a period of 10 generations. The

phenotypes are the result of appropriate expression of the transgene in the endothelium of microvasculature in the adult Tie1-AT1R TG mice (Fig. 2). The TG23+/− and TG26+/− and TG26+/+ mice estimated to contain 10, 1, and 2 transgene copies are normal overall. TG23+/+ mice were not viable, the cause of which is unknown, and examination of the pups reveals normal morphology and organ development. We do not, at present, have any additional information relevant to potential lethality of high-copy Tie1-AT1R transgene expression. The TG6 line with 18 nonexpressing transgene copies is indistinguishable from NT mice. We conclude that the phenotypes described here, common to expressing TG lines, are caused by EC-restricted expression of the activated AT1R rather than disruption of unknown gene(s) resulting from random integration of the transgene(s).

The angiotensinergic stimulation of the endothelium, a potential mechanism involved in normal blood pressure regulation, could be compromised in hypertension. Because the currently available AT1R antagonists do not discriminate cell types, it has not been possible to define the specific function of EC-AT1R from the overall effects of vascular AT1R in pathophysiology. Therefore, the phenotypes of the mouse model described here are pertinent to our understanding of human physiology.

The Tie1-AT1R mice, TG23 and TG26, are hypotensive (Fig. 3*A*), and they demonstrated an attenuated pressor response to infused doses of Ang II (Fig. 3*B*). The Tie1-AT1R transgene expression was detected in the resistance vessels (Fig. 2). The vascular phenotypic differences between NTL and TG were abolished by AT1R blockade with L-158809 as well as by L-NAME (Fig. 3 *C* and *D*), which establishes that hypotension is caused by the transgenic receptor rather than being a nonspecific effect resulting from embryonic developmental changes in vascular structure and function. Furthermore, if these phenotypes are caused by an unknown, aberrant functional property of the constitutively active $AT_{1\text{-}N111G}$ mutant receptor, then the difference between NTL and TG mice would not have been suppressed by AT1R blockade with L-158809.

The data suggest that a single transgene copy is sufficient to lower the setting of systolic blood pressure significantly. The degree of hypotension, in the three lines examined, showed a tendency toward but not strictly proportional to transgene copy numbers, implying that other *in vivo* mechanisms involved in blood pressure regulation compensate for the augmented Tie1-AT1R transgene(s). Hypotension was found in mice lacking the AT1R, angiotensin-converting enzyme, and angiotensinogen (20–22). In contrast, overexpression of Ang II-generating RAS components, such as angiotensinogen, vascular renin (23), and vascular chymase (24), causes hypertension. Increasing AT1R gene dosage, three to four copies per diploid genome, causes hypertension in mice (25). Hypotension observed during EC-targeted overexpression of the AT1R reported here in the mouse model is pertinent because it confirms previous observations on cultured ECs that could not be conclusively proven *in vivo*. There is evidence suggesting that the endothelial AT1R is antagonistic to vasoconstriction; for example, Ang II-evoked constriction is more exaggerated in endothelium-denuded aorta and carotid artery than in the presence of endothelium (12, 13, 26). Functional AT1R is found in acutely isolated and cultured EC, which are coupled to production of various vasorelaxant substances (4, 5, 8).

Significant bradycardia observed in the Tie1-AT1R TG mice raised the possibility that altered cardiac functions underlie hypotension in these mice. The cardiac function determined by echocardiography did not show any differences between TG and NTL. Their hearts show normal histology, and the heart/body weight ratios do not differ. Hypotension and bradycardia have been observed in EC-specific connexin43-null mice (27). Hypertension and bradycardia are also reported in eNOS-null mice (28). Bradycardia in rats (29), dogs (30), and humans (31) given a NOS inhibitor have been reported. On the basis of similarities to these models, we speculated that NO production by eNOS could play a direct role in the phenotypes in our TG mice. We confirmed the dependence of bradycardia on transgene by demonstrating rescue of the symptom by the AT1R-selective antagonist. Furthermore, the elevated circulating NO and expression of eNOS in the TG mice (Fig. 4) are consistent with activation of the endogenous vasorelaxation pathway (32) and elevated blood NO and cGMP levels (Table 1). Although both AT1R antagonist and L-NAME treatment decreased blood NO level and eNOS activity, only AT1R antagonist treatment altered the accompanying bradycardia in TG mice. Possible other mechanisms of bradycardia, baroreceptor, and the electrical conduction system of the heart have not been determined in this work.

The present findings demonstrate that EC-AT1R moderates VSMC-AT1R-mediated vasoconstriction by the RAS in regulating arterial blood pressure. Thus, the resting vascular tone is the net result of opposing activities of EC-AT1R and VSMC-AT1R in this model. In general, the normal blood pressure setting may rely on chronic activation of EC-AT1R by Ang II to limit the magnitude of VSMC constriction to any stimulus. Excessive EC activation could increase NO, which is a potent agonist for production of numerous growth factors, cytokines, and chemokines in ECs (33), thus creating a milieu that can amplify pathogenicity in the blood as well as cells of the vessel wall, including endothelium and smooth muscle cells (33). Compromised EC-AT1R functions may predispose individuals to excessive VSMC stimulation observed in diseases, including hypertension, preeclampsia, unstable angina, atherosclerosis, congestive heart failure, and oxidative stress, which are linked to cardiovascular disease fatalities.

In summary, our transgenic study provides hitherto unforeseen, physiological insights on EC-AT1R functions in an integrated vascular system. Are there blood vessel beds where one should expect a vasodilatation in response to Ang II? These questions are important, and they need answers in further investigations on this experimental model as well as in human studies.

Materials and Methods

Animal Use. Mice were cared for in accordance with the *Guide for the Care and Use of Laboratory Animals* (40) in our Biological Resources Unit. All mice experimental protocols described were reviewed and approved by the Animal Care and Use Committee at the Cleveland Clinic Foundation (CCF).

Generation of Tie1-AT1R TG Mice. The mouse tyrosine kinase receptor (Tie1) promoter (ref. 14; a gift from Kari Alitalo, University of Helsinki, Finland) was amplified by PCR and cloned in front of synthetic rat AT1R and N111G mutant genes (15) with 1D4 epitope. The linear DNA fragment as shown in Fig. 1*A* is referred to as the transgene hereafter. The transgene fragment was injected into the pronuclei of one-cell B6/CBA (Jackson Laboratory, Bar Harbor, ME) mouse embryos, which were surgically implanted into "pseudopregnant" female mice. Founder Tie-AT1R mice were identified by transgene-specific PCR, and progeny were genotyped by Southern blotting (for conditions and primers, see *SI Methods*).

Quantitative RT-PCR. Poly(A)$^+$ RNA was reverse transcribed by using random hexamer priming. The *Taq*Man probe for quantitative real-time PCR of mouse AT1R was from Applied Biosystems, Foster City, CA. The transgene-specific *Taq*Man probe complement to 3′ untranslated region of the transgene (Fig. 1*A*) was synthesized by the Gene Expression Core Facility at CCF.

Membrane Preparation and Radioligand-Binding Experiments. Total membranes isolated from tissues were used in saturation binding

analysis using ^{125}I-[Sar^1,Ile^8]Ang II as the radioligand as described in ref. 15.

Cell Culture and Transfection. BAECs from passage 10 were transfected with expression vectors containing the Tie1-AT$_{1\text{-WT}}$ or the Tie-AT$_{1\text{-N111G}}$ mutant genes. The receptor expression was assessed in each case by Western analysis and by ^{125}I-[Sar^1,Ile^8]Ang II binding analysis. (see *SI Methods*).

Immunohistochemistry. General histological and immunohistochemical methods were performed as described in refs. 32 and 33 and *SI Methods*.

Blood Pressure, Ang II Infusion, and Echocardiography. Systolic blood pressure was measured in conscious, trained mice by tail-cuff blood pressure analysis as described in ref. 34 in a blinded fashion.

For the Ang II infusion studies, 6-month-old male mice were anesthetized as described by Lorenz and Robbins (35). Throughout the experiment, heart rate, respiratory efforts, and arterial pressure were monitored, and a steady stream of 100% oxygen was supplied to lungs. A high-fidelity, calibrated, 1.4F transducer-tipped catheter was introduced into the carotid artery for pressure recordings. A second cannula with a PE10 catheter was introduced into the femoral vein for infusing drugs with a constant-flow pump.

Echocardiographic assessments were performed as described in ref. 36 on lightly anesthetized (pentobarbital sodium, 40 mg per kg of body weight) mice.

NOS Activity. NOS activity was assayed in the presence of $CaCl_2$ and calmodulin in homogenized extracts as described in ref. 37 (for details, see *SI Methods*). The activities are expressed in picomoles of citrulline per milligram of protein per minute.

Blood NO, Biochemistry, and Endothelin-1 Levels. Plasma electrolytes, creatinine, and blood urea nitrogen were measured by using a multiparameter autoanalyzer (38). The blood NO level was estimated from the measurement of nitrosyl hemoglobin by electron spin resonance (39). The plasma levels [endothelin-1 by ELISA (R&D Systems, Minneapolis, MN), plasma renin activity by ELISA (DiaSorin, Stillwater, MN), and atrial natriuretic peptide by enzyme immunoassay (SPI Bio; BIO 101, Morgan Irvine, CA)] were measured according to instructions from the manufacturers.

Statistical Analysis. Multiple group comparisons were analyzed by one-way ANOVA followed by a Turkey–Kramer test. Values of $P < 0.05$ were considered statistically significant.

We greatly appreciate the assistance from Monica Dragoman, Dennis Wilk, John Boros, Jingli Zhang, Russell Desnoyer and expert advice from Shin-ichiro Miura. We thank Robin Lewis for assistance in manuscript preparation. This work was funded in part by National Institutes of Health Grants R01 HL57470 and HL064845 (to S.S.K.) and by Established Investigator Award 9940178N from the American Heart Association (to S.S.K.).

1. de Gasparo M, Catt KJ, Inagami T, Wright, JW, Unger T (2000) *Pharmacol Rev* 52:415–472.
2. Dzau VJ (2001) *Hypertension* 37:1047–1052.
3. Goodfriend TL, Elliott ME, Catt KJ (1996) *N Engl J Med* 334:1649–1654.
4. Ko Y, Glodny B, Stier S, Totzke G, Nickenig G, Dusing R, Sachinidis A, Vetter H (1997) *Biochem Pharmacol* 53:417–421.
5. Pueyo ME, Michel JB (1997) *Gen Pharmacol* 29:691–696.
6. Pueyo ME, N′Diaye N, Michel JB (1996) *Br J Pharmacol* 118:79–84.
7. Gimbrone MA, Jr, Alexander RW (1975) *Science* 189:219–220.
8. Saito S, Hirata Y, Emori T, Imai T, Marumo F (1996) *Hypertens Res* 19:201–206.
9. Heinemann A, Wachter CH, Peskar BA, Holzer P (1997) *Br J Pharmacol* 122:975–984.
10. Thorup C, Kornfeld M, Winaver JM, Goligorsky MS, Moore LC (1998) *Pflügers Arch* 435:432–434.
11. Caputo L, Benessiano J, Boulanger CM, Levy BI (1995) *Arterioscler Thromb Vasc Biol* 15:1646–1651.
12. Boulanger CM, Caputo L, Levy BI (1995) *Hypertension* 26:752–757.
13. Zhang J, Van Meel JC, Pfaffendorf M, Zhang J, Van Zwieten PA (1994) *Eur J Pharmacol* 262:247–253.
14. Korhonen J, Lahtinen I, Halmekyto M, Alhonen L, Janne J, Dumont D, Alitalo K (1995) *Blood* 86:1828–1835.
15. Noda K, Feng YH, Liu XP, Saad Y, Husain A, Karnik SS (1996) *Biochemistry* 35:16435–16442.
16. Balmforth AJ, Lee AJ, Warburton P, Donnelly D, Ball SG (1997) *J Biol Chem* 272:4245–4251.
17. Groblewski T, Maigret B, Larguier R, Lombard C, Bonnafous JC, Marie J (1997) *J Biol Chem* 272:1822–1826.
18. Ohashi Y, Kawashima S, Hirata K, Yamashita T, Ishida T, Inoue N, Sakoda T, Kurihara H, Yazaki Y, Yokoyama M (1998) *J Clin Invest* 102:2061–2071.
19. Iljin K, Petrova TV, Veikkola T, Kumar V, Poutanen M, Alitalo K (2002) *FASEB J* 16:1764–1774.
20. Ito M, Oliverio MI, Mannon PJ, Best CF, Maeda N, Smithies O, Coffman TM (1995) *Proc Natl Acad Sci USA* 92:3521–3525.
21. Krege JH, John SW, Langenbach LL, Hodgin JB, Hagaman JR, Bachman ES, Jennette JC, O'Brien DA, Smithies O (1995) *Nature* 375:146–148.
22. Tanimoto K, Sugiyama F, Goto Y, Ishida J, Takimoto E, Yagami K, Fukamizu A, Murakami K (1994) *J Biol Chem* 269:31334–31337.
23. Caron KM, James LR, Kim HS, Morham SG, Sequeira Lopez ML, Gomez RA, Reudelhuber TL, Smithies O (2002) *Proc Natl Acad Sci USA* 99:8248–8252.
24. Ju H, Gros R, You X, Tsang S, Husain M, Rabinovitch M (2001) *Proc Natl Acad Sci USA* 98:7469–7474.
25. Le TH, Kim HS, Allen AM, Spurney RF, Smithies O, Coffman TM (2003) *Hypertension* 42:507–514.
26. Kulkarni PS, Hamid H, Barati M, Butulija D (1999) *Invest Ophthalmol Visual Sci* 40:721–728.
27. Liao Y, Day KH, Damon DN, Duling BR (2001) *Proc Natl Acad Sci USA* 98:9989–9994.
28. Shesely EG, Maeda N, Kim HS, Desai KM, Krege JH, Laubach VE, Sherman PA, Sessa WC, Smithies O (1996) *Proc Natl Acad Sci USA* 93:13176–13181.
29. Widdop RE, Gardiner SM, Kemp PA, Bennett T (1992) *Br J Pharmacol* 105:653–656.
30. Elsner D, Muntze A, Kromer EP, Riegger GA (1992) *Am J Hypertens* 5:288–291.
31. Stamler JS, Loh E, Roddy MA, Currie KE, Creager MA (1994) *Circulation* 89:2035–2040.
32. Rudic RD, Shesely EG, Maeda N, Smithies O, Segal SS, Sessa WC (1998) *J Clin Invest* 101:731–736.
33. Cooke JP, Dzau VJ (1997) *Annu Rev Med* 48:489–509.
34. Krege JH, Hodgin JB, Hagaman JR, Smithies O (1995) *Hypertension* 25:1111–1115.
35. Lorenz JN, Robbins J (1997) *Am J Physiol* 272:H1137–H1146.
36. Tanaka N, Dalton N, Mao L, Rockman HA, Peterson KL, Gottshall KR, Hunter JJ, Chien KR, Ross J, Jr (1996) *Circulation* 94:1109–1117.
37. Schaub FJ, Han DK, Liles WC, Adams LD, Coats SA, Ramachandran RK, Seifert RA, Schwartz SM (2000) *Nat Med* 6:790–796.
38. Nickenig G, Harrison DG (2002) *Circulation* 105:393–396.
39. Landmesser U, Dikalov S, Price SR, McCann L, Fukai T, Holland SM, Mitch WE, Harrison DG (2003) *J Clin Invest* 111:1201–1209.
40. Committee on Care and Use of Laboratory Animals (1985) *Guide for the Care and Use of Laboratory Animals* (Natl Inst Health, Bethesda), DHHS Publ No (NIH) 85-23.